Supplementary Online Materials

Title: *Variability and Reliability in T Cell Activation from Regulated Heterogeneity in Protein Levels*

Authors: Ofer Feinerman, Joël Veiga, Jeffrey Dorfman, Ronald N. Germain, & Grégoire Altan-Bonnet

Supplementary online material SOM#1

Experimental methods:

a) Mice, cell lines, antibodies, and reagents.

Splenocytes and lymphocytes were isolated from C57Bl/6N mice (Taconic Farms, Rockville, MD, USA) or H-2^b OT-1 TCR transgenic mice (NIAID contract colony, Taconic Farms) on a Rag-$2^{-/-}$ background (S*1*) and used to prepare cultures of primary cells (see below). All mice were bred and maintained in accordance with the protocol (MSKCC#05-12-031) approved by the institutional animal care and use committee (IACUC) of Memorial Sloan-Kettering Cancer Center.

L cells transfected with H-$2K^b$ and sorted for high expression levels (a gift of P. Savage) or RMA-S cells (TAP$^{-/-}$ T cell lymphoma expressing H-$2K^b$ (S*2*)) were used as antigen-presenting cells (APCs). The agonist ovalbumin peptide SIINFEKL (OVA) and its variants EIINFEKL and SIIRFEKL (all 95% pure) were obtained through the Keck peptide synthesis facility of Yale University. E10 antibody against ppERK was purchased from Cell Signaling Technology (Beverly, MA, USA); MR9–4(PE) against Vβ5.2, B20.1(PE) against Vα2, 53–6.7(PE) against CD8α, were from BD Biosciences/Pharmingen (San Diego, California, United States); K-23 against ERK1, C-19 against SHP-1, and C-14 against ERK2 were from Santa Cruz Biotechnology (Santa Cruz, CA, USA); YTS169 against CD8α was from Cedarlane Laboratories (Burlington, NC, USA). Anti-CD8α 53–6.7 Fab fragment was prepared by the MSKCC monoclonal antibody core facility. Secondary antibodies (anti-mouse(APC), anti-rabbit(PE) and anti-rat(FITC)) were purchased from Jackson ImmunoResearch Laboratories (West Grove, PA, USA): special care (adsorption on heterologous IgG) was taken care to minimize cross-reactivity. Recombinant IL-2 was purchased from eBioscience (San Diego, CA, USA).

FACS buffer consisted of 10% fetal bovine serum (MSKCC tissue culture core facility) and 0.1% sodium azide in PBS. DAPI was purchased from Dojindo (Gaithersburg, MD, USA). All cell cultures were prepared in complete RPMI prepared by the MSKCC core media preparation facility (this medium contained RPMI-1640 augmented with 10% fetal bovine serum, 10μg/ml penicillin-strep, 2mM glutamine, 10mM HEPES (pH7.0), 1mM sodium pyruvate, 0.1mM non-essential amino acids and 50μM β-mercaptoethanol. Recombinant mouse IL-2 and IL-7 were obtained from eBioscience.

b) Preparation of stimulated primary T lymphocytes.

OT-1 T cell cultures were prepared as follows. C57Bl/6N splenocytes were pulsed for 2hr with 100nM SIINFEKL peptide, then irradiated (3000RAD), washed once and used as stimulator/feeder cells. OT-1 cells were harvested from axillary, brachial and inguinal lymph nodes as well as spleen (splenocytes were treated with ACK lysis buffer to remove red blood cells), and mixed with SIINFEKL-pulsed B6 splenocytes in complete RPMI. After two days, cells were expanded by diluting 2 fold into medium containing 100 pM IL-2. After four days, the cells were again expanded by 2 fold dilution into medium with IL-2. After one more day of culture, cells were harvested and spun through a 1.09 density Ficoll-Paque Plus gradient (GE Healthcare) to remove dead cells. Live cells were recovered, washed twice in complete medium and resuspended at 1 million/ml in complete medium with 100pM IL-2. Cells were used for experiments between 6 and 8 days after primary stimulation.

c) T cell activation and antibody staining protocol.

APCs were pulsed with serial dilutions of OVA or variant peptides for 2 hr at 37°C, then washed with T cell medium at the time of harvest, and resuspended with anti-CD8α (53-6.72)-Fab-coated T cells in their conditioned media in a V-bottom 96-well plate (Corning). Fab-coating was performed 10 min before cell use by incubating T cells with 10 µg/ml of Fab fragment. T:APC cell contacts were synchronized using a quick centrifugal spin (10s at 400g). Plates containing T:APC conjugates were placed on a water bath at 37°C and incubated for 5 min. Supernatants were then discarded, T:APC conjugates disrupted by vortexing, and cells resuspended in ice-cold 4% paraformaldehyde for 15 min. Cells were then permeabilized with ice-cold 90% methanol for 15 min on ice, and washed twice with FACS buffer. Cells were then stained with rabbit-anti-endogenous protein (e.g., to SHP-1) and mouse-anti-ppERK (0.2µg/ml) for 30 min at room temperature. Secondary antibodies [anti-rat(FITC) + anti-rabbit(PE) + (anti-mouse(APC)] were then used at 2 µg/ml for 30min. Cells were loaded in FACS buffer containing 1 µg/ml DAPI and fluorescence acquired on a LSRII instrument (BDBioscience, San Diego, CA, USA), after compensation of fluorescence bleed-through between channels (see SOM#8 for an example of FACS data analysis).

d) Downregulation of SHP-1 expression by siRNA transfection.

OT-1 T cell blasts from *ex vivo* culture were harvested 5 days post-stimulation, washed in PBS, and resuspended in Nucleofector solution (Amaxa) with or without 20nmol of SHP-1 siRNA (Dharmacon). Electroporation was performed according to Amaxa protocol for mouse splenocytes (e.g., using the X-01 program), except that cells were placed in complete RPMI medium augmented with 100pMol of recombinant IL-2 and 100pMol recombinant IL-7. Electroporated cells were then rested for 24 to 48hr before use.

e) Data processing and fitting.

- Fit for the ppERK dose-response.

To determine plateau and EC_{50} of the ppERK dose-response of T cells, we used a three-parameter fit:

$$\%ppERK^{+}\left(\left[OVA\right]\right) = Bckg + \left(Plateau - Bckg\right) * \frac{\left[OVA\right]}{\left[OVA\right] + EC_{50}},$$

where *Bckg* is the background response (corresponding to *[OVA]*=0). All fits were performed using Matlab and were considered valid if their Pearson coefficient *R* was greater than 0.98.

- Subgating for different levels of signaling proteins and fit of dose-response.

To assess the phenotypic variability of the T cell response (based on differential expression of a signaling molecule *X*), we used a Matlab program. First, for each experimental set, we confirmed that the antibody staining for *X* was independent of activation (fluctuations of geometric mean fluorescence intensity M.F.I. were within 10% of the mean comparing unstimulated and activated T cells). Second, we sorted the data based on the geometric MFI of the *X* staining, and binned the samples into 30 gates

containing equal number of cells. We then tabulated the Geometric Mean Fluorescence Intensity of *X* and the average ppERK response for each subgate and for each quantity of peptide. This produced 30 dose responses (Figure 2B) that were fit as described in the previous paragraph.

The same analysis was performed with two-dimensional subgating for different levels of CD8 and SHP-1.

- Fit of (SHP-1,CD8) distribution.

To assess the potential correlation in the levels of expression of endogenous signaling proteins (e.g., CD8 and SHP-1), we computed the 2D histogram of the logarithmic fluorescence intensity (as measured by FACS analysis). We then fit this 2D histogram with a 2D-lognormal distribution:

$$f(x,y) = \frac{1}{2\pi\sigma_x\sigma_y}\exp\left(-\frac{1}{2(1-\rho^2)}\left(\frac{x^2}{\sigma_x^2}+\frac{y^2}{\sigma_y^2}-\frac{2\rho xy}{\sigma_x\sigma_y}\right)\right), \quad (1)$$

where ρ is the correlation between x and y. The covariance matrix is, in this case:

$$\Sigma = \begin{pmatrix} \sigma_x^2 & \rho\sigma_x\sigma_y \\ \rho\sigma_x\sigma_y & \sigma_y^2 \end{pmatrix}.$$

Typically, for the histogram in Figure 3C, σ_x=0.27, σ_y=0.15 and ρ=0.48. The quality of the fit was estimated using χ^2 goodness-of-fit criteria (S*3*) (standard deviations for the histogram data were estimated by compiling 6 samples of 10000 cells: we checked that the square-root of the frequency in each bin is an accurate estimate of this standard deviation as predicted for a Poisson distribution). Typically, for the histogram in Figure 3C, χ^2=1300 for ν=1370 degrees of freedom (number of non-empty bins minus 3 fitting parameters).

Diagonilizing the covariance matrix yields the eigenmode of correlation between SHP-1 and CD8 levels with [CD8] $\propto$ ([SHP-1])$^{0.4}$. We find that the distribution for the variable x=[CD8]/([SHP-1])$^{0.4}$ is relatively narrow with a coefficient of variation η=0.3 compared to the wider distribution in CD8 and SHP-1 levels considered alone (η=3.5 and 0.6 respectively) (Figure 3C).

For the uncorrelated distribution (Figure 3D – right panel), the covariance matrix is null, and there is no eigenmode to be represented.

- Fit of EC_{50}([SHP-1],[CD8]) dependence.

As suggested by our computer model for the dependence of ppERK EC_{50} on different levels of CD8 and SHP-1, we fit our data with power laws:

$$\log_{10}\left(ec_{50}([SHP-1],[CD8])/Mol\right) = \alpha\log_{10}[SHP-1] + \beta\log_{10}[CD8] + \delta. \quad (2)$$

For the map in Figure 3B, α=+2.5, β=-4.6, δ=-9.60. The goodness-of-fit criteria was satisfied as χ^2=141 for ν=170 degrees of freedom (173 non-empty bins minus 3 fitting parameters). Note that the standard deviation for each $\log_{10}(ec_{50}/\mathrm{Mol})$ was estimated to be between 1 and 2, because of noise in antigen presentation by L cells and a limited number of cells in individual bins (especially in the outer borders of the (SHP-1,CD8) distributions)

- Estimating the distribution of EC_{50} with or without correlation in (SHP-1,CD8) levels.

To estimate the distribution *D* of EC_{50}, for a distribution *f* of SHP-1 and CD8, we used equations (1) and (2):

$$D(EC_{50}) = \iint dxdy\big(f(x,y)\big)_{ec_{50}(x,y)=EC_{50}}.$$

From this distribution, we could estimate the coefficient of variation of EC_{50} for a natural distribution of SHP-1 and CD8 (as in Figure 3C) or for a bi-lognormal distribution of SHP-1 and CD8 with the same individual coefficients of variation but without co-regulation (see SOM #9).

f) Computer modeling of the early events in T cell signaling.

The computer model used in this study was presented earlier (S*4*). Please refer to this publication for details and to download the Matlab file. Note that no modification of our original model was necessary to account for the phenotypic variability of T cell ligand response that we document here experimentally.

The model comprises a set of ordinary differential equations that encapsulates the biochemical dynamics of ligand-receptor interactions and enzymatic activities. We did not include stochasticity in the chemical reactions of the model given that most of the relevant enzymes in T lymphocytes have high levels of expression (for example, [ERK1]=10μMol because $V_{cytoplasm}\approx 90$fl (Altan-Bonnet et al. 2005)). The match between our deterministic model predictions and experimental results does preclude the role of intrinsic fluctuations in chemical reactions as a source of variability in response.

Supplementary online material SOM#2:

Time-lapse imaging or flow cytometric analysis of cells genetically tagged using GFP is the most common method used to study biological flexibility at the single-cell level (S*5-10*).However, this approach is not practical when seeking to analyze how endogenous variation in signaling components affects the behavior of primary mammalian cells *ex vivo*. Thus we first validated a combination of antibody staining and flow cytometry as a quantitative method to assess the heterogeneity of expression of signaling components within a population of primary T cells. To do so, we first estimated the noise associated with the measurement of protein expression levels by this method. We found such measurements to be highly accurate, with a coefficient of variation of $\eta_{measurement}<0.15$ (see below). Second, we tested polyclonal antibodies against key signaling components identified by our model and validated three antibodies for accurate measurements of endogenous levels of proteins in mouse T cells in flow cytometry applications (see SOM#3).

Estimate of the measurement noise for levels of expression of membrane proteins

To estimate the noise associated with measuring protein levels, we took advantage of the well-documented correlation of expression of CD8α and CD8β on the surface of primary T lymphocytes. We stained non-permeabilized OT-1 T cell blasts with anti-CD8α(APC) and anti-CD8β(PE) antibodies and confirmed the known linear correlation between the expression of these two proteins on the membranes

of effector T cells (Figure S1.A). We then measured the coefficient of variation[1] η for the ratio of fluorescence intensity (f_{CD8a} and f_{CD8a}) associated with antibody staining, corresponding to different levels (l_{CD8a} and l_{CD8a}) of coreceptors (Figure S1B).

As $\eta\left(f_{CD8\alpha}/f_{CD8\beta}\right)=\sqrt{\eta^2_{measurement}+\eta^2\left(l_{CD8\alpha}/l_{CD8\beta}\right)}\Rightarrow \eta_{measurement}\le\eta\left(f_{CD8\alpha}/f_{CD8\beta}\right)$,

In other words, $\eta(f_{CD8a}/f_{CD8b})$ constitutes an upper bound for the coefficient of variation $\eta_{\text{measurement}}$ of the noise associated with antibody measurement of membrane proteins.

For membrane proteins, $\eta_{measurement}\le 0.11$.

Supplementary online material SOM#3:

Estimate of the measurement noise for levels of expression of intracellular proteins.

Our methodology relies on our ability to characterize T cells at the individual cell level, in order to assess cell variability in the expression of key signaling components and its effect on cell responsiveness. Hence, we needed to check that classical protocols of immunocytochemistry (FACS staining) were adequate to probe cell-to-cell variability in the expression of cytoplasmic enzymes.

Phoenix cells were transfected with Mouse Stem Cell Virus (MSCV) expressing GFP. One day after transfection, cells were harvested and fixed with 4% paraformaldehyde, permeabilized with 0.1% saponin, and stained intracellularly with anti-GFP antibody (Roche) + anti-mouse antibody (Cy5) (Jackson Immunochemicals). The correlation between the expression levels (as measured by the natural fluorescence of GFP) and the staining levels (measured by Cy5 fluorescence) is linear over 3 decades of GFP expression. The distribution (for a given GFP level) in Cy5 staining has a coefficient of variation of less than 13% (Figure S2). This noise estimate does not depend whether one uses monoclonal (from mouse or goat) or polyclonal (from rabbit) antibodies and the corresponding secondary antibodies [our unpublished data].

Using our estimate of η_{noise}<13% for the assessment of the measurement noise associated with intracellular staining and FACS analysis (Figure SOM), we could deconvolve the coefficient of variation $\eta_{protein}$ (or equivalently the typical standard deviation $\sigma_{protein}$) for the distribution of intracellular proteins in T lymphocytes when measuring η_{staining} for the distribution of staining of intracellular proteins. Taking into account that all distributions are lognormal, we computed:

$$\sigma_{protein}=\sqrt{\sigma^2_{staining}-\sigma^2_{noise}}\ \ with\ \sigma_i=\sqrt{\ln\left(1+\left(\frac{\eta_i}{100}\right)^2\right)}.$$

This formula shows that, with $\eta_{noise}\approx$13%, our immunochemistry protocol yields an accurate estimate of the natural variability of expression levels of proteins when $\eta_{staining}$ > 20% (Figure S2.B). Typically, we report coefficients of variation $\eta_{staining}$ between 30 and 60%; thus we estimated 26%< $\eta_{protein}$ <57% (Figure S2.B). In other words, the natural distribution of the levels of expression of cytoplasmic proteins is sufficiently wide to allow accurate estimate by immunocytochemistry.

[1] The coefficient of variation η is defined as the ratio of the standard deviation and the mean of a distribution (in linear scale). For a typical FACS staining, η =50%, 85% of the recorded fluorescence intensity *I* falls between </>/2 and </>*2 (where </> is the mode of the distribution).

Supplementary online material SOM#4:

a) Validation of ppERK FACS measurement by comparison with Western blot measurement.

To validate a phospho-specific antibody for individual cell measurement, we checked that FACS and Western blot measurements yielded comparable results (Figure S3). Cells were activated with antigen-presenting cells (APC) that had been pulsed with a serial dilution of agonist peptide and paraformaldehyde-fixed before activation (fixation of APC insures that only T cells get lysed in the subsequent step). T cells were then either lysed with 1% NP40-containing buffer or fixed/permeabilized with 4% paraformaldehyde/90% methanol. Lysates were run on 13%-PAGE and transferred onto PVDF, and stained with the phospho-specific antibody of interest. In parallel, fixed/permeabilized cells were stained intracellularly with the same antibody and other markers to distinguish T cells from APC. We then compared the phospho-specific signals obtained on the western blot and on the FACS profile. We present in Figure S3 our validation of a mouse monoclonal antibody raised against ERK-pTpY (E10 antibody from Cell Signaling Technology).

b) Validation of FACS measurement of the levels of endogenous proteins.

To validate a polyclonal antibody for FACS detection of endogenous protein levels, we relied on RNAi downregulation for the gene of interest. OT-1 T cell blasts were transfected with siRNA using Amaxa nucleofector technology (see Methods SOM#1). We then tested the antibody of interest by checking that it yielded quantitative agreement for the effects of gene downregulation when measured by Western blot of cell lysates and by FACS staining. We present in Figure S4 our validation of a rabbit polyclonal antibody raised against SHP-1 (C-19 from Santa Cruz Biotechnology).

A second important validation for our experimental protocols is the consistency of staining during cell activation. Indeed, we are interested in measuring the endogenous levels of signaling proteins that are involved during cell activation, but measurements of intracellular protein levels are done after activation. We checked also that the epitope of interest was not altered during cell activation, *i.e,.* that antibody staining yielded a reliable activation-independent measurement of the level of the protein of interest (Figure S4).

Checklist to validate an antibody for FACS application.

To summarize, here are the three criteria that must be satisfied to validate an antibody for our single-cell analysis of signaling responses:

- ✓ The antibody should yield a single band in a western blot assay
- ✓ Delivering siRNA against the mRNA of a protein of interest should yield a measurable downregulation of the protein that is identical when estimated by Western Blot and or by FACS.
- ✓ Antibody staining must yield a FACS measurement of the level of a protein of interest that is activation-independent.

Only 30% of antibodies (out of 14 tested) that commercial suppliers distribute for FACS applications passed our validation tests.

Supplementary online material SOM#5:

Validation of Fab(53.6-7) to tag available CD8α before activation

We used the Fab fragment of the 53.6-7 anti-CD8α antibody to tag CD8α before activation. This antibody has been documented as non-blocking in functional assays or in K^b/OVA tetramer binding assays (S*11, 12*). However, we needed to check that its tagging would not affect T cell responsiveness in our ppERK assay.

OT-1 T cell blasts were incubated for 10 min at room temperature with or without 10 μg/ml of Fab(53.6-7). These cells were then activated as described in SOM#1, fixed, permeabilized and stained for ppERK. In Figure S5, we compare the dose-response for ppERK phosphorylation for OT-1 T cells that had been tagged or not with Fab. The exact match of the two dose-response curves establishes that use of anti-CD8α Fab fragment antibody pre-staining does not perturb the ppERK response of T cells and allows us to monitor the number of available membrane-bound CD8α at the time of activation.

Supplementary online material SOM#6:

Complete single-cell analysis of T cell signaling response

In this section, we present the raw FACS profiles for the ppERK response of OT-1 T cells after 5 min of contact with APCs pulsed with different concentrations of OVA (an agonist peptide). First, T cells were gated based on their light scattering (Forward scattering vs side-Scattering – Figure S6.1). Second, cells were gated for their DNA content (as estimated by intracellular DAPI staining) to eliminate doublets and apoptotic cells. Third, we checked the homogeneity of the gated population (Figure S6.2) as demonstrated by the lognormality of its CD8α or X staining (where X can be ERK-1 or SHP-1).

FACS profiles show the correlated ppERK response for different levels of CD8α and SHP-1 (Figure S6.3). Cells expressing lower levels of SHP-1 have a higher frequency of ppERK response and cells expressing higher levels of SHP-1 have a lower frequency of ppERK response: this confirms that SHP-1 acts a digital-sensitive controller of OT-1 T cell response (Figure 1). For CD8α, cells expressing higher levels tend to switch from null to full ppERK response at lower concentrations of antigens compared to cells expressing lower levels of CD8α: this confirms that CD8α acts as a positive analog-sensitive controller of ppERK response (Figure 1). ERK1 levels do not help segregate between higher or lower responsiveness for T cells and hence ERK1 was characterized as a non-critical signaling component.

Supplementary online material SOM#7:

Activation of OT-1 blasts under Fab blocking of CD8

Variability in the expression levels of CD8 is limited for primary T cells (CV<30%; Figure 2A), while our computer model predicts that downregulation larger than 10-fold is required to perturb the

efficiency of TCR signaling (Figure S7). We achieved large tonic interference with CD8 availability on OT-1 T cells by titrating YTS169 Fab fragment that blocks CD8α binding (S*13*). We calibrated the extent of CD8α blocking by calibrating the amount of YTS169 Fab fragment that decorated the cells at the time of activation (Figure S7). We then recorded ppERK responses for different doses of antigen and different levels of available CD8α. We found that varying levels of available CD8α strongly affected the EC_{50} of the dose response (200-fold increase for 20-fold decrease of the number of available CD8α), while maintaining the overall response of the cells. Hence, we experimentally confirmed that the TCR signaling machinery is analog-sensitive to CD8α levels. This experiment is consistent with our single-cell analysis of T cell responsiveness for different levels of CD8α.

Supplementary online material SOM#8:

Computer predictions for the effect of varied expression of signaling protein on the minimal number (EC_{50}) of ligands required to activate ppERK response.

In Figure S8, we present predictions for a non-agonist (τ =2.5s), a weak agonist (τ =4.6s), an agonist (τ =8.5s) and a strong agonist ligand (τ =16s). Differences within the observed physiologic range in CD8 and SHP-1 expression [see Fig. 2A] are predicted to affect ligand discrimination, with CD8 variation having an analog effect on EC_{50} and SHP-1 having mostly a digital effect on the response frequency. Variation in the ERK levels is predicted not to affect T cell response.

Supplementary online material SOM#9:

(SHP-1,CD8) coregulation limits the variability of T cell response.

We estimated the distribution of EC_{50} for OT-1 blasts responding to agonist ligands K^b/SIINFEKL, for the natural distribution of CD8 and SHP-1 or for an hypothetical distribution where CD8 and SHP-1 levels are uncorrelated (see SOM #1e for details on the computation). For the natural distribution of signaling proteins (Figure 3D – left panel), we found that the distribution of EC_{50} was lognormal with a coefficient of variation of 5.0 (Figure S9 - blue curve). For a hypothetical distribution of CD8 and SHP-1, with the same individual distributions but without co-regulation the distribution of EC_{50} would also be lognormal but with a larger coefficient of variation of 18 (Figure S9 – red curve)

Supplementary online material SOM#10:

Response to non-agonist ligands is limited to $CD8^{high}SHP\text{-}1^{low}$ T cells.

We tested the responsiveness of OT-1 T cells towards L mouse fibroblasts expressing H-$2K^b$ MHC that had been pulsed with a maximal dose of 100nMol of EIINFEKL peptide. This peptide/MHC complex has been previously documented to drive OT-1 thymocyte differentiation (positive selection); it is also an antagonist of OT-1 activation for mature T cells in the periphery (S1). In other words, K^b/EIINFEKL is a non-agonist ligand for OT-1 T cell blasts that is the closest to being an agonist ligand.

We measured the activation of OT-1 as described in the protocol SOM#1 and report here the fraction of responding cells for different levels of CD8 and SHP-1 (Figure S10). Only cells with high CD8 and low SHP-1 levels mount a robust ppERK response.

As in Figure 3, we note that the natural co-regulation in CD8 and SHP-1 levels in OT-1 T cell blasts is aligned with the isoclines of ppERK response. In other words, co-regulation of CD8 and SHP-1 levels limits the number of cells that spuriously get activated by this non-agonist ligand. This result remains qualitative as the limited potency of K^b/EIINFEKL yields truncated dose-response and does not allow us to estimate EC_{50} or response frequency of OT-1 blasts for this particular ligand.

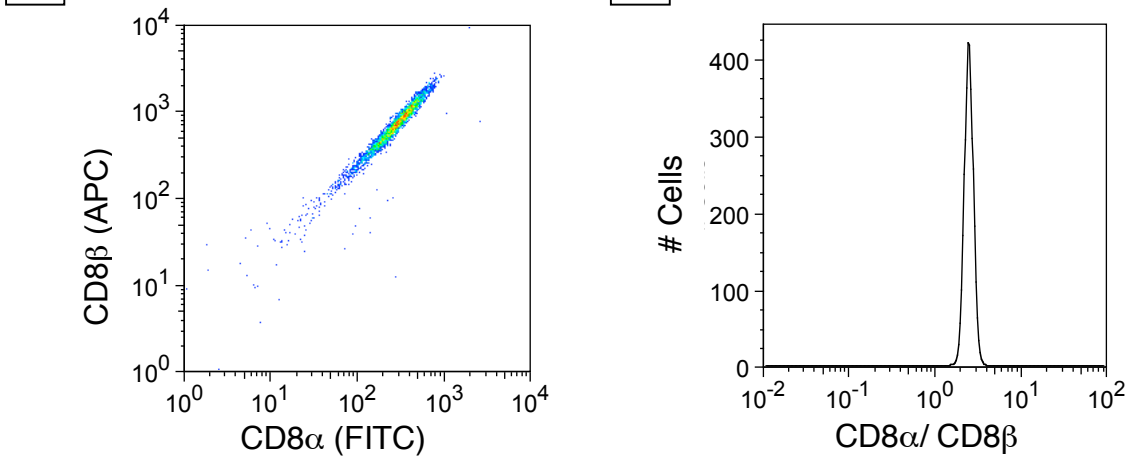

Figure S1. Estimate of the noise associated with estimation of the levels of expression of surface proteins by immunocytochemistry. A) CD8α and CD8β levels were measured by FACS after surface staining of OT-1 T cell blasts with anti-CD8α (FITC) and anti-CD8β (APC): these CD8 levels are linearly correlated. B) Measuring the distribution of CD8α/CD8β yields an upper bound for the noise associated with surface protein measurement by FACS: the coefficient of variation for this noise is η_{noise}<0.11. See SOM#2 for details.

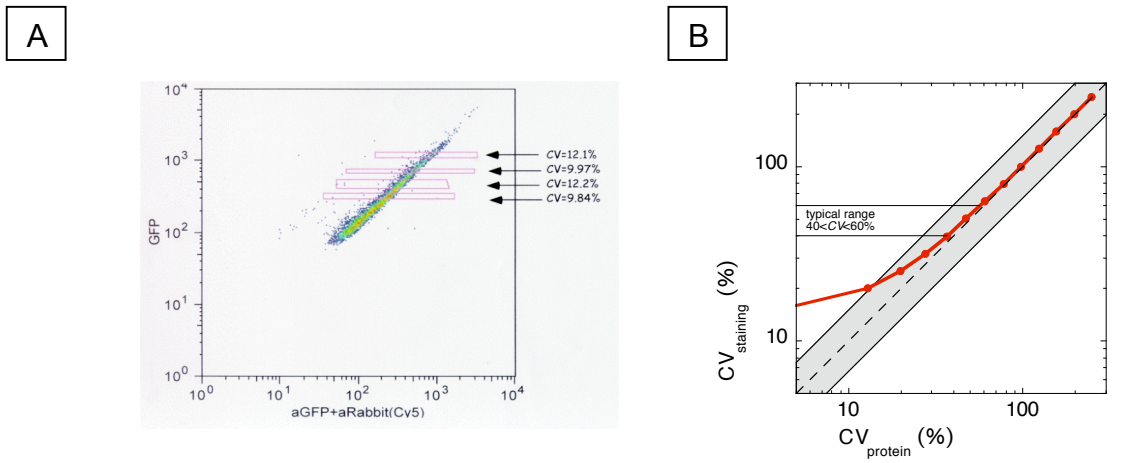

Figure S2 Linearity of immunocytochemistry and distribution of protein expression in T lymphocytes. A) Phoenix cells were transfected with a retrovirus expressing GFP and stained with the combination of anti-GFP antibody and anti-rabbit(Cy5). The limited variability in dual-antibody staining fluorescence compared to the absolute number of GFP molecules (as measured by their intrinsic fluorescence) sets an upper bound to the noise incurred by our immunocytochemistry protocol to a coefficient of variation η_{noise}<13%. B) Theoretical correlation between the coefficient of variation for the distribution of levels of expression of a protein ($\eta_{protein}$), and its measurement by immunocytochemistry ($\eta_{staining}$). The dash line represents equality $\eta_{protein}$ =$\eta_{staining}$. The grey area represents 50% confidence. See SOM#3 for details.

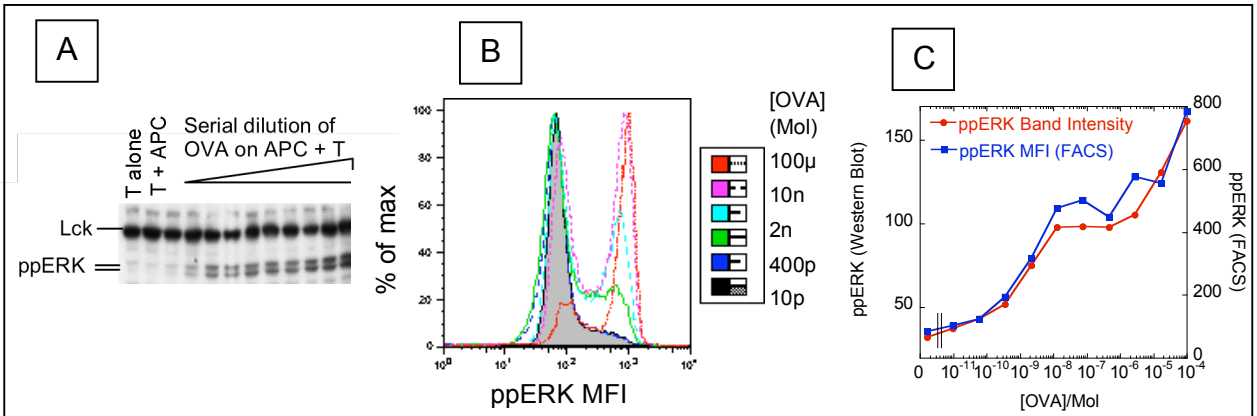

Figure S3. Validation of FACS measurement for phosphorylated ERK (ppERK), by comparison with Western Blot measurement. OT-1 T cells were activated for 3min by RMA/s, pulsed with varying amounts of OVA peptide, and fixed. A) Lysates of OT-1 and RMA/s cells, resolved by denaturing polyacrylamide gel electrophoresis, transferred onto PVDF membrane and immunoblotted with αppERK (E10 monoclonal) and αLck (polyclonal) antibodies. B) FACS histogram of the ppERK intracellular staining of the same OT-1 T cells (after fixation and permeabilization, instead of lysis). C) Comparison of the dose-response curves for ppERK, as measured by Western Blot (optical density of the ppERK bands, normalized by the optical density of the Lck band) or by FACS (mean fluorescence intensity of antibody staining). See SOM#4 for details.

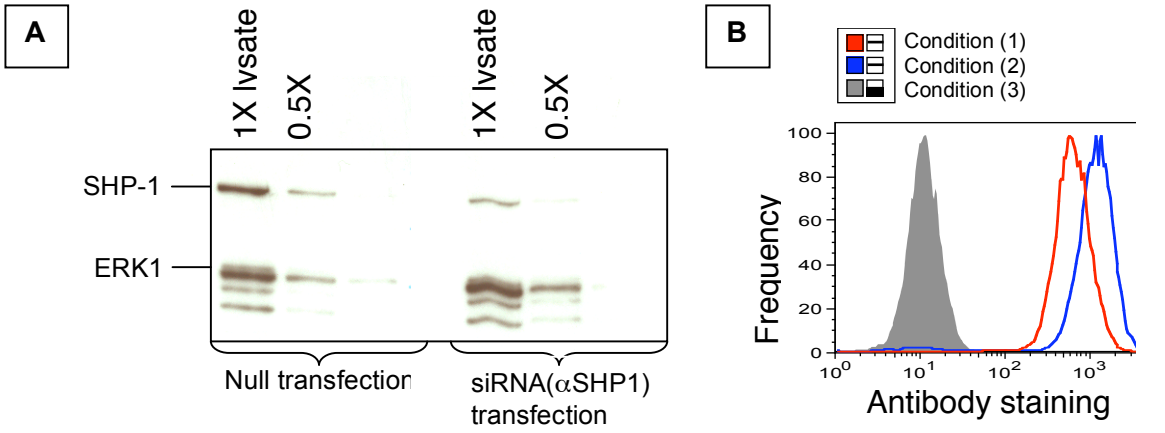

Figure S4. Validation of antibody against endogenous protein for FACS application. We compare the staining for SHP-1 in OT-1 T cell blasts after null-transfection or after transfection with SHP-1 specific siRNA. A) Western blot of cell lysates shows a 2.5 downregulation of SHP-1 after siRNA transfection. B) FACS analysis of fixed/permeabilized cells shows a 2.1 fold downregulation of SHP-1 staining [Condition (1): SHP-1 staining of siRNA(SHP-1) transfected cells; condition (2): SHP-1 staining of null-transfected cells; condition (3): IgG control staining of null-transfected cells]. The concordance of FACS and western blot measurements proves that this anti-SHP-1 antibody yields quantitative estimate of SHP-1 levels in T cells. See SOM#4 for details.

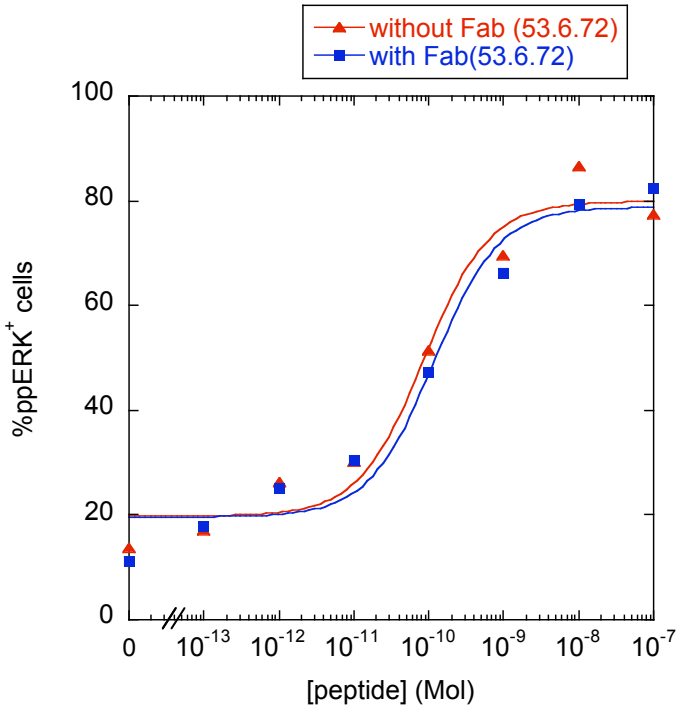

Figure S5. Anti-CD8α-Fab(53.6-7) fragment does not interfere with ppERK response. See SOM#5 for details.

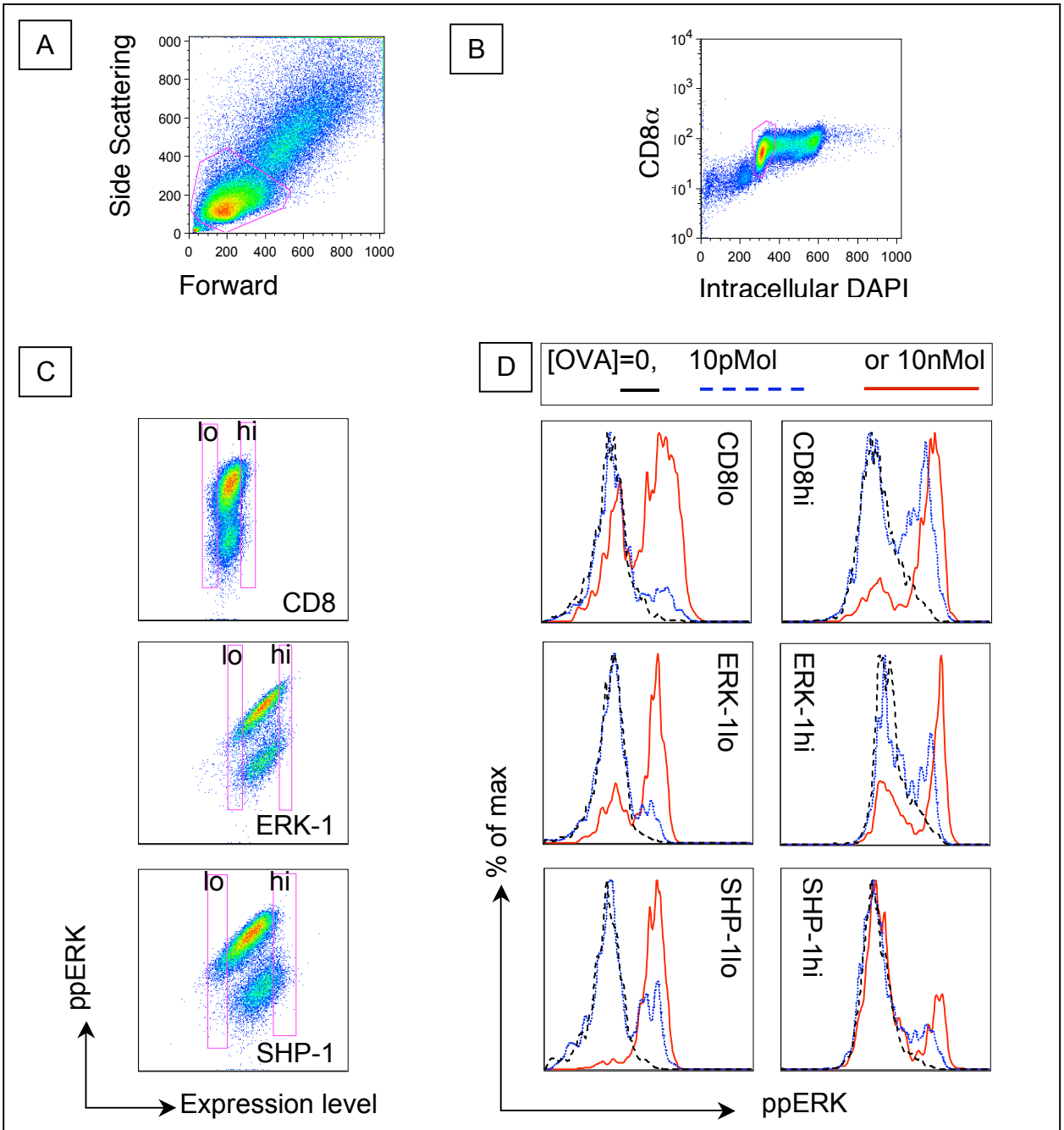

Figure S6.1. FACS analysis of individual T cells (this figure corresponds to the experiment presented in Figure 2). See SOM#6 for details.

A) Gating in forward/side scatter dot plot isolates T cells from antigen-presenting L cells (these cells are larger in size). B) Sub-gating in DAPI/CD8a staining selects live/singlet cells. Our intracellular staining for DNA content enables us to distinguish singlet cells (DAPI=2n with a mean fluorescence intensity at 300) from doublet (DAPI=4n with a mean fluorescence intensity at 570). Apoptotic cells are gated out as $CD8a^{-}DAPI<2n$ cells (mean fluorescence intensity below 290). C) Final scatter plot for ppERK vs (CD8 or ERK-1 or SHP-1) staining in T cells (here under strong activation). D) Histograms of ppERK response for the subgates defined in C for three different concentrations of OVA showing that cell responsiveness varies with the levels of expression of CD8 and SHP-1 but not ERK-1.

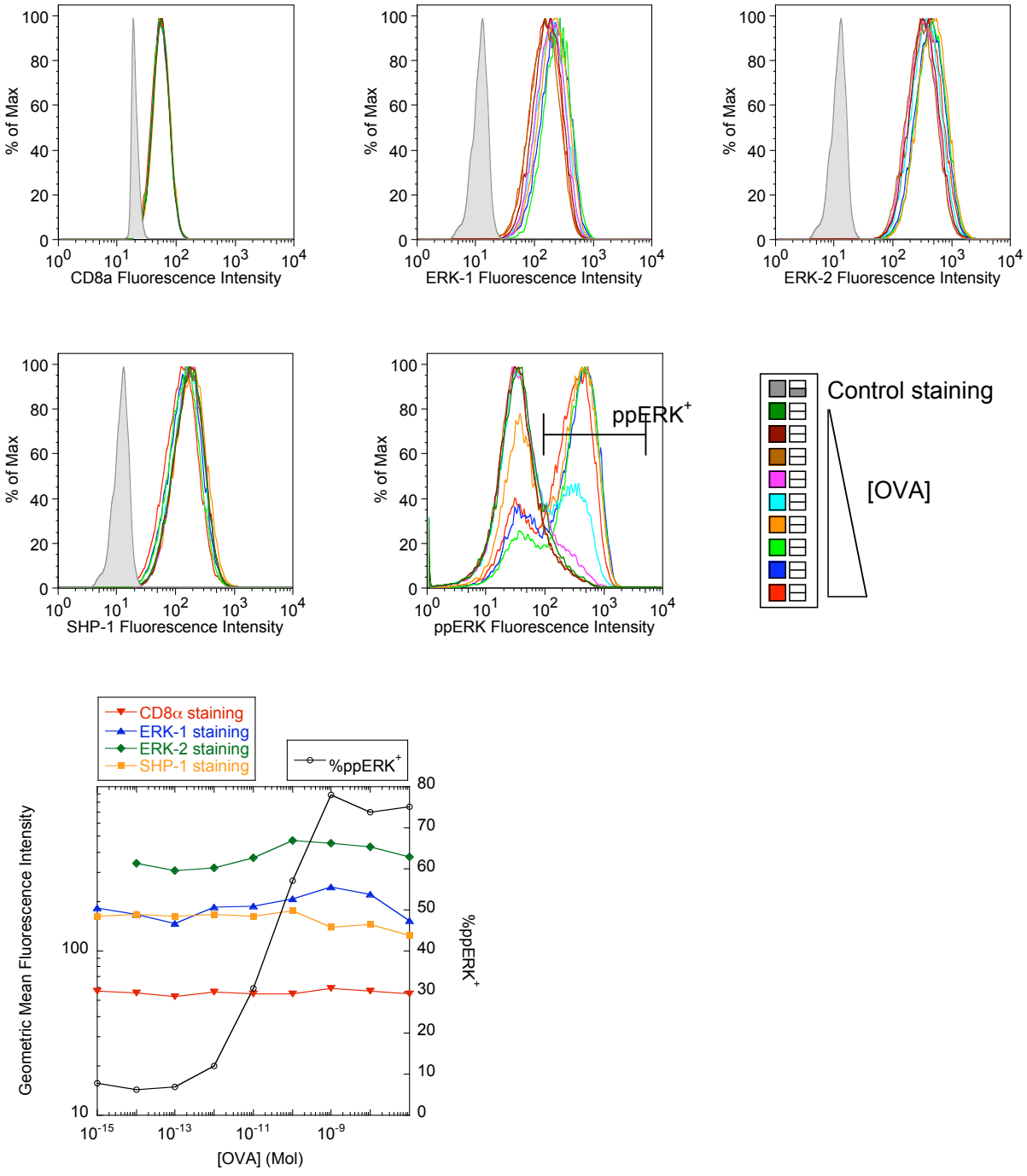

Figure S6.2. Validation of the constant staining for CD8α, ERK-1 and SHP-1 for T cells undergoing activation. These data correspond to the experiment presented in Figure 1. We present these histograms to show that staining is constant despite different levels of activation (associated with different quantities of OVA peptide). Control staining for CD8α is the staining with the secondary anti-rat(FITC) antibody alone; control staining for ERK-1and SHP-1 is the staining with irrelevant rabbit IgG and secondary anti-rabbit(PE) antibodies. See SOM#6 for details.

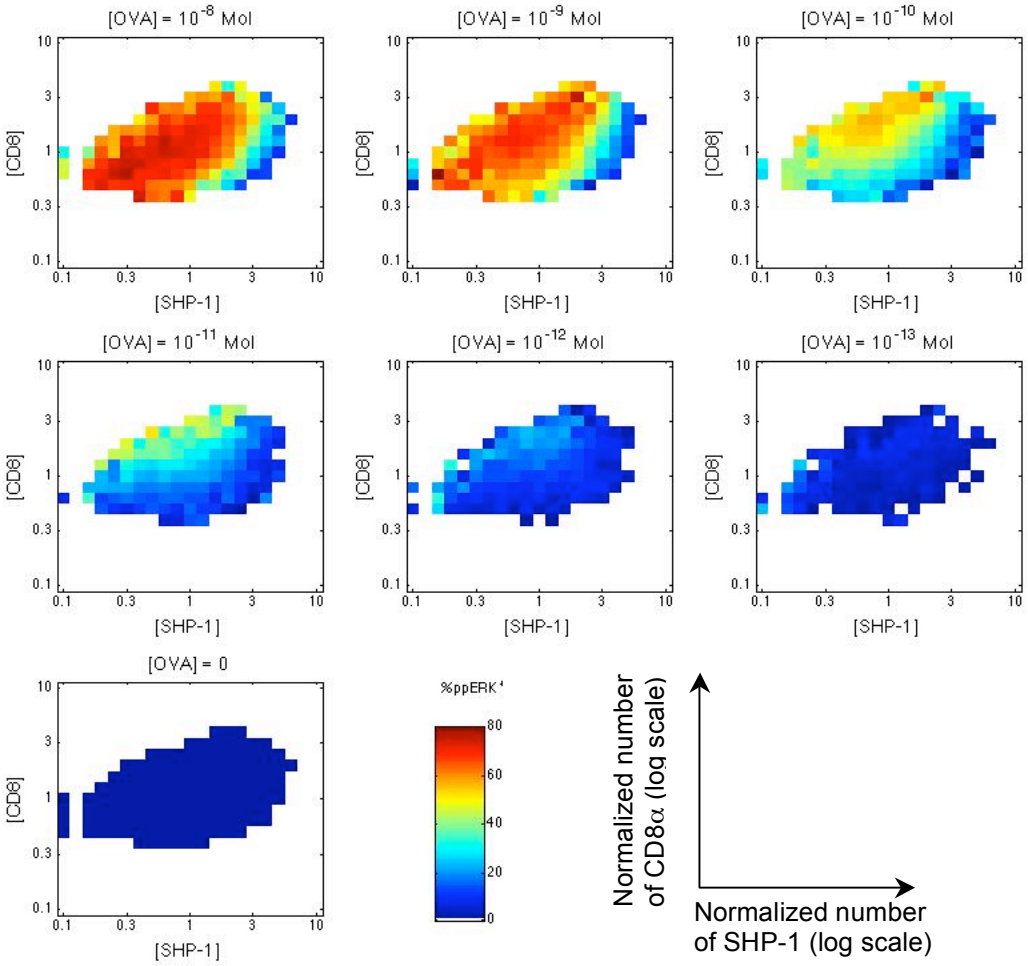

Figure S6.3: ppERK response of OT-1 T cell blasts to L-K^b cells pulsed with varying concentrations of OVA agonist peptide. These images display the color-coded frequency of responding cells (%ppERK$^+$), for different levels of SHP-1 and CD8α. See SOM#6 for details.

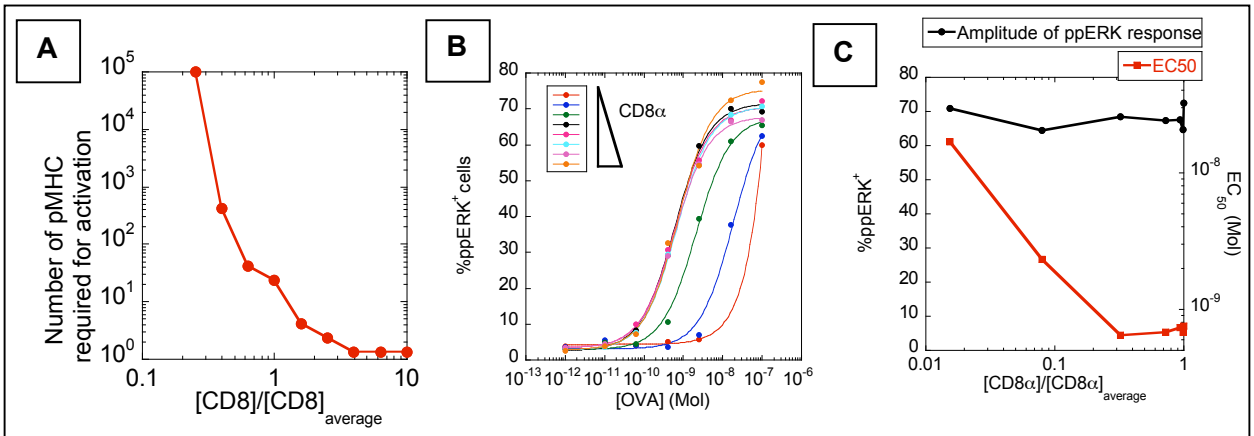

Figure S7. Testing OT-1 ppERK response after CD8α-blocking with YTS169 Fab fragment. A) Prediction from computer model. B) Dose-response of OT-1 ppERK response after 5 min of activation with SIINFEKL-pulsed RMA/S, for different amount of available CD8α. C) Inhibition of ppERK responsiveness in OT-1 cells upon blocking of CD8α. The characteristic concentration EC_{50} of activating peptides (and not the amplitude of the response) depends on the number of available (unblocked) CD8α. See SOM#7 for details.

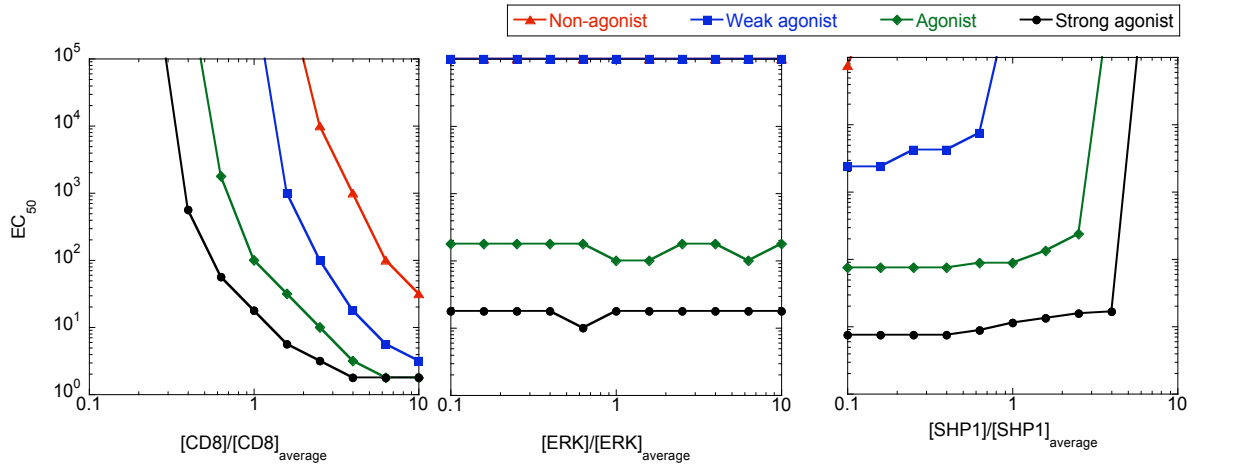

Figure S8: computer predictions for the effect of varied expression of signaling protein on the minimal number (EC_{50}) of ligands of varied quality that are required to activate ppERK response. See SOM#8 for details.

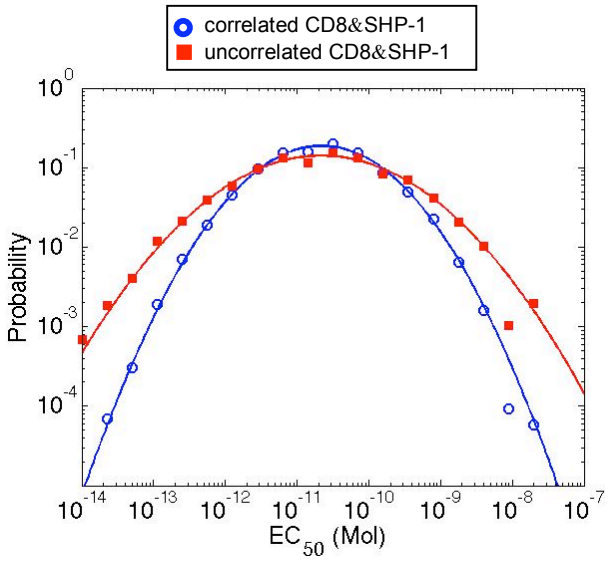

Figure S9: distribution of EC_{50} for natural (correlated) distribution of CD8&SHP-1 expression or for an uncorrelated distribution of CD8 & SHP-1. See SOM#9 for details.

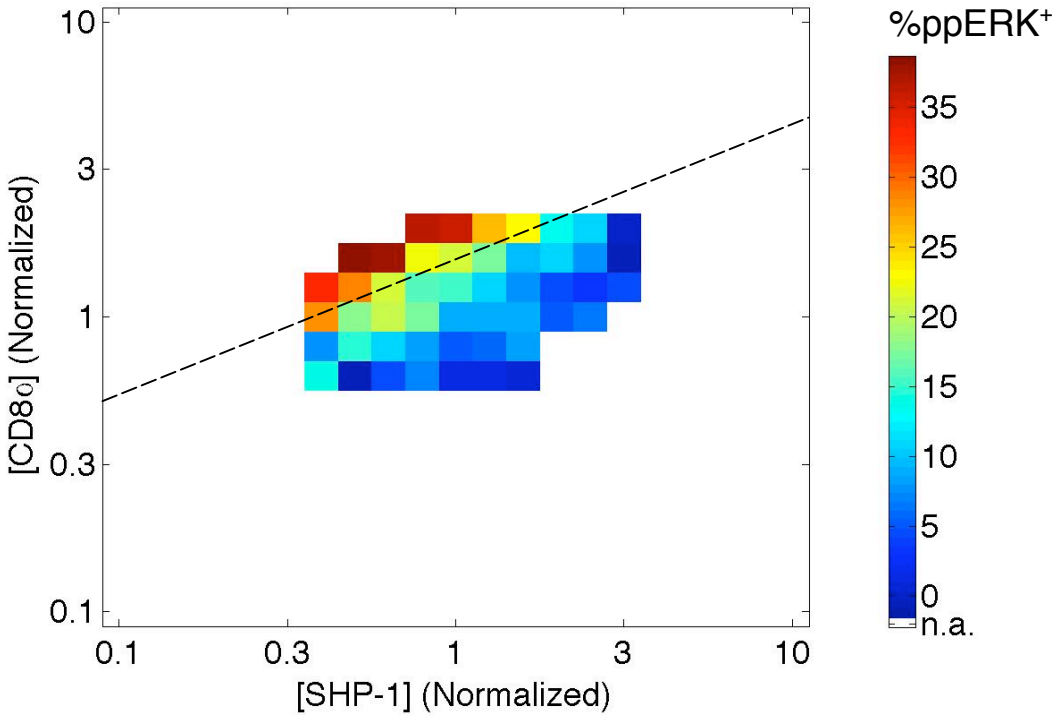

Figure S10: ppERK response of OT-1 T cell blasts to the maximal dose of non-agonist ligands (K^b/EIINFEKL) for different levels of SHP-1 and CD8. Note how only cells for with $[CD8]/([SHP-1])^{0.5}>2$ (dashed line) respond significantly with $\%ppERK^+>20\%$. These cells would potentially be more prone to trigger an auto-immune response, by spuriously getting activating with a large dose of non-agonist ligands. See SOM#10 for details.

References:

S1. K. A. Hogquist et al., Cell 76, 17 (1994).
S2. A. Townsend et al., Nature 340, 443 (1989).
S3. P. R. Bevington, D. K. Robinson, Data Reduction and Error Analysis for the Physical Sciences. (WCB McGraw-Hill, Boston, 1992), pp. 195-220
S4. G. Altan-Bonnet, R. N. Germain, PLoS Biol 3, e356 (2005).
S5. A. Bar-Even et al., Nat Genet 38, 636 (2006).
S6. A. Becskei, B. B. Kaufmann, A. van Oudenaarden, Nat Genet 37, 937 (2005).
S7. J. R. Newman et al., Nature 441, 840 (2006).
S8. A. Sigal et al., Nature 444, 643 (2006).
S9. M. B. Elowitz, A. J. Levine, E. D. Siggia, P. S. Swain, Science 297, 1183 (2002).
S10. J. M. Raser, E. K. O'Shea, Science 304, 1811 (2004).
S11. M. A. Daniels, S. C. Jameson, J Exp Med 191, 335 (2000).
S12. L. Devine, M. E. Hodsdon, M. A. Daniels, S. C. Jameson, P. B. Kavathas, Immunol Lett 93, 123 (2004).
S13. G. E. Kwan-Lim, T. Ong, F. Aosai, H. Stauss, R. Zamoyska, Int Immunol 5, 1219 (1993).